BUTTERWORTH HEINEMANN

Polymer Vol. 36 No. 14, pp. 2745–2751, 1995

0032-3861/95/$10.00+0.00

Gas transport properties of polyarylates based on 9,9-bis(4-hydroxyphenyl)anthrone

M. R. Pixton and D. R. Paul*
Department of Chemical Engineering and Center for Polymer Research, The University of Texas at Austin, Austin, TX 78712, USA
(Received 9 January 1995)

Gas transport of helium, hydrogen, oxygen, nitrogen, methane and carbon dioxide gases in two polyarylates based on 9,9-bis(4-hydroxyphenyl)anthrone and isophthalic acid or t-butyl isophthalic acid has been examined. Substitution of a t-butyl group on the isophthalate ring increases polymer permeability two- to three-fold, primarily due to higher diffusion coefficients. The physical properties of these materials are very similar to those of their fluorene bisphenol-based analogues; however, the former are more permselective but less permeable than the latter. The favourable interaction of CO_2 with the anthronylidene carbonyl unit and the higher degree of polarity in the repeat unit apparently contribute to these differences.

(Keywords: gas permeation; polyarylates; tertiary butyl group; membranes)

INTRODUCTION

Previous studies have shown that some polyarylates combine attractive gas transport properties with high glass transition temperatures, resistance to hydrocarbon solvents and good film forming properties, making them interesting candidate materials for membrane separation processes[1–4]. As a continuation of our previous work, this paper reports on two polyarylates based on 9,9-bis(4-hydroxyphenyl)anthrone (PhAnth) and isophthalic acid or 5-tertiary butyl isophthalic acid. Vinogradova *et al.*[5] and Morgan[2] have shown that polymers based on PhAnth are amorphous and have very similar physical properties to their fluorene bisphenol (FBP)-based analogues. Gas transport properties, however, are expected to differ somewhat. The presence of a carbonyl unit in the connector group should enhance PhAnth-based polymer permselectivity by increasing the polar interactions between polymer chains and with some penetrant molecules, as compared with the FBP-based analogues. The t-butyl group substitution on the isophthalate unit and the large anthronylidene connector group should disrupt chain packing and, thus, increase gas permeability at the cost of decreased permselectivity. By combining these two effects, it is hypothesized that improved gas transport properties, relative to those of the FBP-based polymers, may be obtained for some separations.

EXPERIMENTAL

9,9-Bis(4-hydroxyphenyl)anthrone was synthesized by condensing phenol and anthraquinone in the presence of tin(IV) chloride. 5-tertiary Butyl isophthalic acid obtained from Amoco Chemical Company was converted to the diacid chloride by reaction with thionyl chloride. Isophthaloyl dichloride was purchased from Aldrich Chemical Company. The PhAnth-based polyarylates described here were synthesized in our laboratory via solution polycondensation reactions as described by Morgan[2,6,7]. Data for two analogous polyarylates based on FBP are included for comparison[3]. The polymer structures and their abbreviations are listed in *Table 1*.

Polymer films of 50–100 μm thickness were prepared by casting filtered solutions containing ~5 wt% of each polymer in chloroform onto glass plates at room temperature. After most of the solvent had evaporated, the films were stripped from the glass plates and then vacuum dried, first at room temperature for 24 h and then at incrementally higher temperatures until 150°C was reached after about 4 days. The films were held above 150°C for at least 24 h and then removed from the vacuum oven. Thermogravimetric analysis (t.g.a.) with a Perkin–Elmer TGA-7 verified complete solvent removal from the vacuum dried films. The glass transition temperature (T_g) of each polymer was measured using a Perkin–Elmer DSC-7 differential scanning colorimeter (d.s.c.) at a heating rate of 20°C min^{-1}. Dynamic mechanical thermal analysis (d.m.t.a.) was performed using a Polymer Laboratories DMTA operated at a frequency of 3 Hz from −150 to 200°C at a heating rate of 4°C min^{-1}.

Wide-angle X-ray diffraction (WAXD) scans were made for each polymer using a Phillips APD 3520 X-ray diffractometer at a Cu Kα wavelength of 1.54 Å. The corresponding d-spacings were calculated from the diffraction peak maxima using the Bragg equation, $n\lambda = 2d \sin\theta$. Polymer densities (ρ) were measured in a density gradient column based on degassed, aqueous solutions of calcium nitrate at 30°C. The intrinsic viscosities ([η]) in chloroform at 25°C were measured

* To whom correspondence should be addressed

Table 1 Phenolanthrone-based polyarylate structures and physical properties

Polymer abbreviation	Structure[a] R_1	R_2	T_g (°C)	T_γ (°C)	ρ (g cm^{-3})	d-spacing (Å)	FFV[b]	$[\eta]$[c] (dl g^{-1})
PhAnth/IA	d	H	293	−68	1.263	4.8, 7.3	0.162	0.84
PhAnth/tBIA	d	t-butyl	297	−73	1.185	5.2, 7.8	0.178	1.19
FBP/IA	e	H	296	−66	1.222	4.8, 6.7	0.180	0.88
FBP/tBIA	e	t-butyl	297	−82	1.146	5.0, 7.3	0.192	1.09

[a] The general polyarylate structure is as follows:

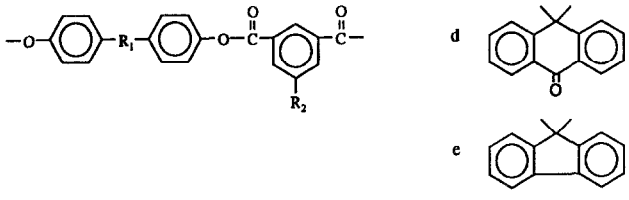

[b] *FFV* calculated using the methods of Bondi and Van Krevelen

using a size 25 Cannon–Fenske capillary viscometer as an indication of molecular weight.

Pure gas permeability coefficients for He, H_2, O_2, N_2, CH_4 and CO_2 gases were measured in a pressure-rise type permeation cell at 35°C using the standard techniques employed in our laboratory[8]. All the gases were chromatography grade with the exception of CH_4 which was chemically pure grade. H_2 and O_2 permeabilities were measured up to 2 atm while He, N_2, CH_4 and CO_2 permeabilities were measured up to 20 atm upstream pressure. CO_2 permeation was measured last to avoid the time-dependent hysteretic effects that have been associated with CO_2 pressurization and depressurization cycles[9,10]. Ideal permselectivities ($\alpha^*_{A/B}$) were calculated from

$$\alpha^*_{A/B} = \frac{P_A}{P_B} \quad (1)$$

where P_A and P_B are the permeabilities of pure gases A and B. Pure gas sorption of O_2 at pressures up to 5 atm and N_2, CH_4 and CO_2 at pressures up to 35 atm were measured in a two volume pressure decay type sorption cell at 35°C[11,12].

RESULTS AND DISCUSSION

The physical properties of these polyarylates are listed in *Table 1*. Each formed clear, tough films with adequate mechanical strength for permeation testing. The T_g of PhAnth/tBIA is only 4°C higher than that of PhAnth/IA. The T_gs of the two FBP-based polymers are virtually identical and very close to those of their PhAnth-based analogues. A previous study[3] showed that for the bisphenol A-based isophthalate, addition of a t-butyl group increased the T_g by 35°C. For large, bulky connector groups such as anthronylidene, molecular motions are already suppressed and the addition of a t-butyl group does not greatly increase the T_g of the PhAnth/tBIA polymer.

The WAXD scans for the two PhAnth-based polyarylates show two broad diffraction peaks similar to those previously reported for the FBP-based polymers. The most prominent peak, located near 5 Å, has been attributed to the average chain spacing while the secondary peak has been attributed to the alignment of aromatic connector groups on adjacent polymer chains to form loose 'stacks'[3,13,14]. It is the average spacing between these 'stacks' rather than the individual polymer chain spacings that accounts for the secondary peak. It appears from these data that aromatic connector group stacking is significant in the PhAnth-based polyarylates. The most prominent WAXD peak in each spectrum was selected as representative of the average polymer chain d-spacing and is listed first in the d-spacing column of *Table 1*. The primary d-spacing, based on the most prominent WAXD peak, is greater for PhAnth/tBIA than for the PhAnth/IA. This increase in d-spacing is also reflected in the lower density of PhAnth/tBIA. The primary d-spacings of the PhAnth-based polymers are the same or slightly higher than those of the FBP-based analogues while the secondary d-spacings are higher. The slightly larger size of the anthronylidene connector is probably responsible for these differences.

The measured polymer densities were used to calculate fractional free volume (FFV) from[15,16]

$$FFV = \frac{V - V_0}{V} \quad (2)$$

where V is the measured specific volume and V_0 is the occupied volume of the polymer. The occupied volume is estimated from the van der Waals' volume (V_w) according to the relation

$$V_0 = 1.3V_w \quad (3)$$

The van der Waals' volume of the 9,9′-anthronylidene group was estimated from Bondi's tabulations as 99.4 cm^3 mol^{-1}. The calculated polymer fractional free volumes are listed in *Table 1*. As noted in previous papers, FFV is increased by the addition of t-butyl

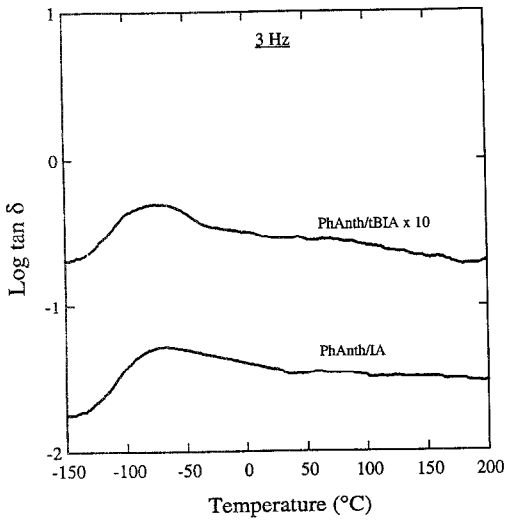

Figure 1 Tan δ at 3 Hz as a function of temperature for the polyarylates. The curve for the PhAnth/IA material corresponds to the tan δ scale shown. The curve for PhAnth/tBIA has been shifted upwards by a factor of 10 for clarity

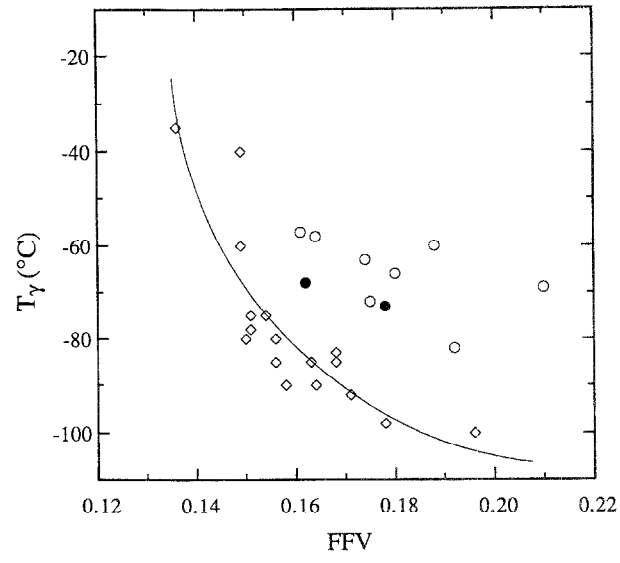

Figure 2 Relationship between the sub-T_g relaxation temperature, T_γ, and fractional free volume. Solid circles represent the PhAnth data while the open symbols are for polyarylates[3] (circles) and polysulfones[17–21] (diamonds) described elsewhere. The line represents the best fit of the polysulfone data

groups to the isophthalate unit of aromatic polyesters. It is seen here that *FFV* is lower for the PhAnth-based polymers than for their FBP-based analogue. Increased polar attractions between chains is the probable explanation for this effect.

The d.m.t.a. traces for the PhAnth-based polyarylates are shown in *Figure 1*, the temperature at which the sub-T_g gamma relaxation occurs, i.e. T_γ, being summarized in *Table 1*, the tan δ peaks in the gamma region are similar in size but the isophthalate polymer has a broader peak than the t-butyl substituted material. t-Butyl substitution lowers the T_γ transition temperature for both the PhAnth and FBP-based polyarylates. Since t-butyl substitution also increases chain *d*-spacing and *FFV*, it follows that lower intermolecular barriers to rotation, due to larger chain spacings, are the primary cause for the observed decrease in T_γ. The T_γ transition temperatures are higher for the PhAnth-based polyarylates than for the FBP-based analogues. A previous study showed that large, non-polar, cross planar connector groups do not hinder bisphenol phenyl ring rotational mobility but, in fact, do lower rotational barriers by increasing polymer *FFV*[3]. The introduction of polar or polarizable groups on to the polymer backbone can, however, increase intermolecular attractions and, thus, rotational barriers. This effect is illustrated by the higher T_γ of the PhAnth-based polymers as compared with the FBP-based analogues. *Figure 2* shows a plot of T_γ *versus FFV* for the PhAnth-based materials plus a number of other polyarylates[3] and polysulfones[17–21]. The current data correlate reasonably well with the results for the polyarylates studied previously.

Pure gas permeability coefficients and ideal selectivities for gas pairs of particular interest are shown in *Table 2*. Pure gas permeability isotherms as a function of upstream driving pressure are given in *Figures 3* and *4*. The permeability coefficients for the larger gases decrease with increasing upstream pressure as expected for glassy polymers and as predicted by the frequently used dual-mode sorption model. The effect of t-butyl substitution is to increase the permeability of PhAnth/tBIA about two- to three-fold compared with PhAnth/IA. For the O_2/N_2, He/CH_4 and CO_2/CH_4 gas pairs, the PhAnth-based polymers have higher selectivities than their FBP-based analogues but lower levels of permeability. This trade-off is shown graphically for O_2/N_2 in *Figure 5* and CO_2/CH_4 in *Figure 6*. The O_2/N_2 separation properties of PhAnth/IA are slightly above the curve drawn as a guide for illustrating the typical 'trade-off' for this set of polyarylates. PhAnth/IA is significantly more selective for both O_2/N_2 and CO_2/CH_4 separations than its FBP-based analogue. This improvement probably stems, in part, from the effects of increased polar interactions on chain

Table 2 Gas permeability and ideal gas separation factors at 35°C[a]

Polymer	P_{O_2}[b] (barrers)	$\alpha^*_{O_2/N_2}$[b]	P_{CO_2} (barrers)	$\alpha^*_{CO_2/CH_4}$	P_{He} (barrers)	α^*_{He/CH_4}
PhAnth/IA	2.05	5.74	9.0	27.0	18.0	54.0
PhAnth/tBIA	6.82	5.05	25.9	17.3	38.1	25.4
FBP/IA	3.03	5.32	12.4	20.1	22.3	36.2
FBP/tBIA	9.55	4.95	36.8	15.5	45.9	19.3

[a] Data at 10 atm
[b] Data at 2 atm

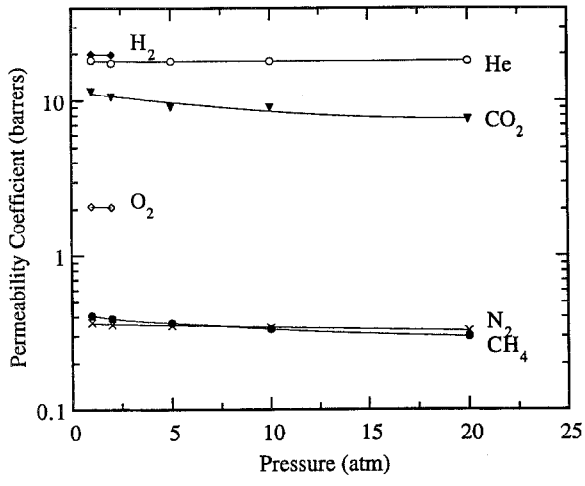

Figure 3 Pressure dependence of PhAnth/IA permeability coefficients at 35°C

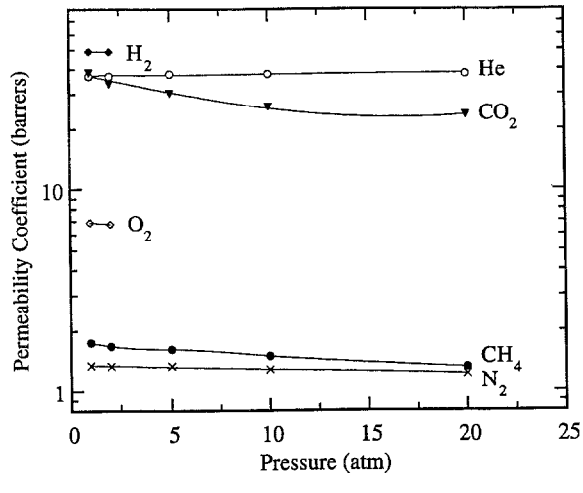

Figure 4 Pressure dependence of PhAnth/tBIA permeability coefficients at 35°C

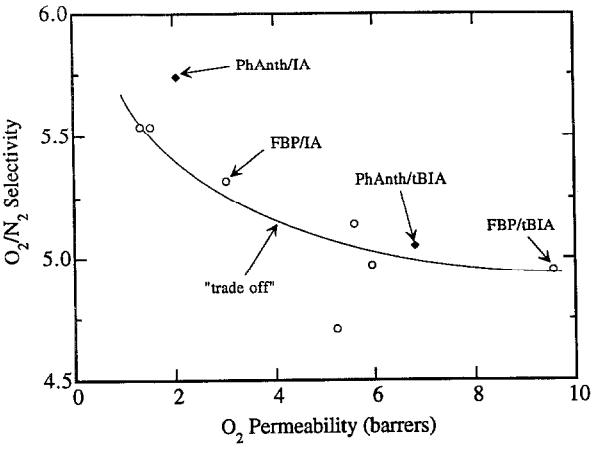

Figure 5 Effect of bisphenol monomer structure and t-butyl substitution on oxygen permeability and oxygen/nitrogen selectivity. Solid diamonds represent the PhAnth data while the open circles are for polyarylates described elsewhere[3]. The curve shown was drawn as a guide for illustrating the typical 'trade-off' for this set of polymers

packing and motion that influence transport, plus, in the case of CO_2/CH_4, the favourable interaction of CO_2 with the anthronylidene carbonyl group that can significantly improve overall permselectivity.

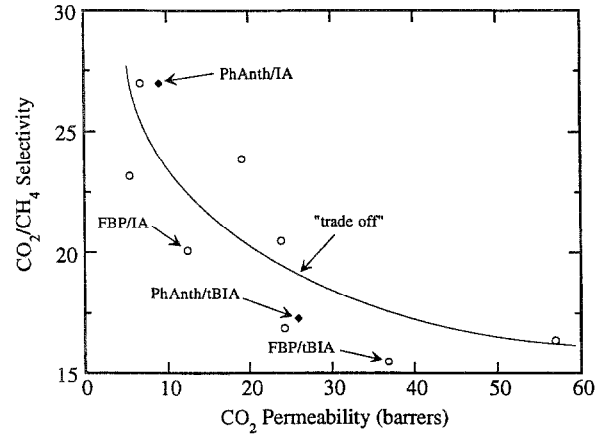

Figure 6 Effect of bisphenol monomer structure and t-butyl substitution on carbon dioxide permeability and carbon dioxide/methane selectivity. Solid diamonds represent the PhAnth data while the open circles are for polyarylates described elsewhere[3]. The curve shown was drawn as a guide for illustrating the typical 'trade-off' for this set of polymers

Previous studies[19,20] have shown a correlation between gas permeability, P, and fractional free volume, FFV, of the form

$$P = A\exp\left(\frac{-B}{FFV}\right) \tag{4}$$

where the parameters A and B depend on temperature and gas type but not on polymer type. *Figure 7* shows a semi-logarithmic plot of O_2 permeability *versus* inverse FFV for these polyarylates along with data for a number of other polyarylates and polysulfones. The correlation of these data, in the form suggested by equation (4), is quite good considering the wide diversity of the polymer structures represented.

Pure gas sorption isotherms for N_2, CH_4 and CO_2 are shown in *Figure 8* for PhAnth/IA and *Figure 9* for

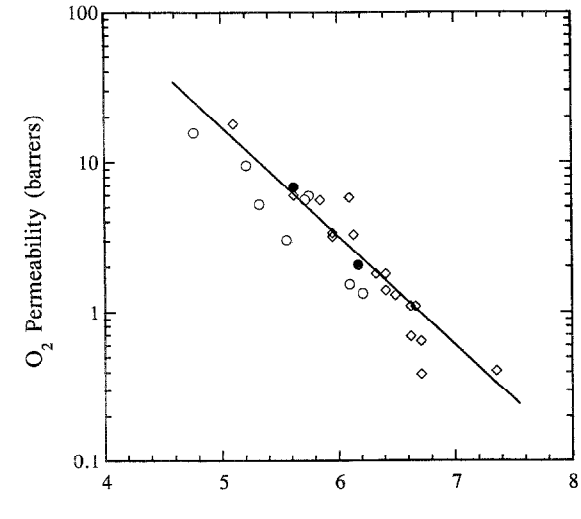

Figure 7 Correlation of oxygen permeability with inverse fractional free volume. Solid points represent the current polyarylate data while open points correspond to various polyarylates[3] (circles) and polysulfones[17–21] (diamonds) described elsewhere. The line is the best linear fit to the polysulfone data

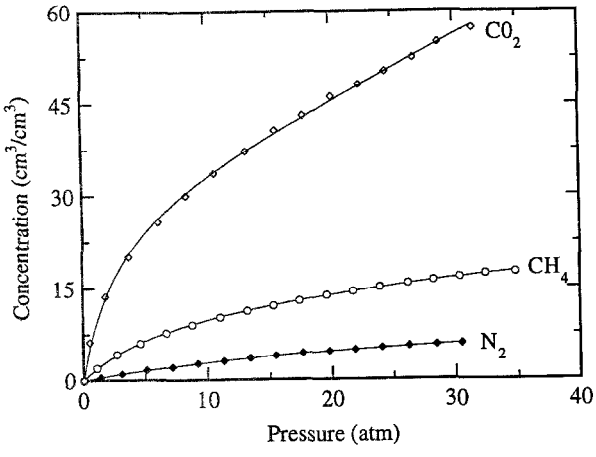

Figure 8 Sorption isotherms for nitrogen, methane and carbon dioxide in PhAnth/IA at 35°C

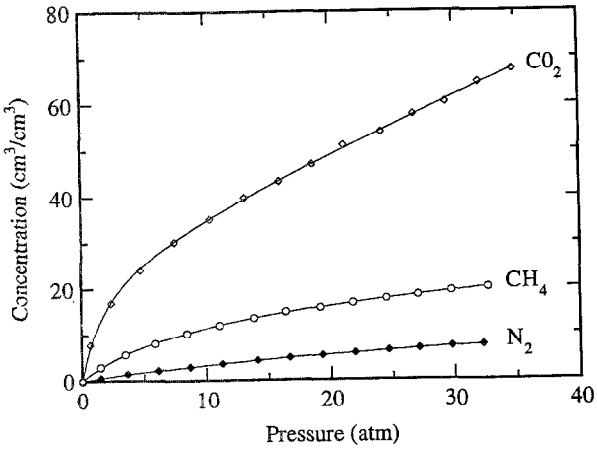

Figure 9 Sorption isotherms for nitrogen, methane and carbon dioxide in PhAnth/tBIA at 35°C

PhAnth/tBIA. The relative contributions of solubility and diffusivity to overall gas permeability can be calculated from

$$P = \bar{D}\bar{S} \tag{5}$$

where $\bar{D}$ is the concentration-averaged diffusion or mobility coefficient and $\bar{S}$ is the solubility coefficient calculated from the secant slope of the sorption isotherm evaluated at the upstream condition. The ideal overall permselectivity (equation (1)) can be factored into solubility and diffusivity terms using equation (5) to give

$$\alpha^*_{A/B} = \frac{P_A}{P_B} = \left(\frac{\bar{D}_A}{\bar{D}_B}\right)\left(\frac{\bar{S}_A}{\bar{S}_B}\right) \tag{6}$$

where $(\bar{D}_A/\bar{D}_B)$ is the mobility selectivity and $(\bar{S}_A/\bar{S}_B)$ is the solubility selectivity. The O_2 and CO_2 solubility and diffusivity coefficients as well as the calculated solubility and mobility selectivities for the gas pairs O_2/N_2 and CO_2/CH_4 are reported in *Tables 3* and *4*. t-Butyl substitution increases oxygen solubility while the solubility selectivity for O_2/N_2 remains approximately the same. The diffusivity of each gas is increased by the t-butyl substitution, but diffusivity selectivity is reduced. The oxygen solubility is lower in all the PhAnth-based polyarylates while both the solubility and diffusivity selectivity for O_2/N_2 are higher for PhAnth/IA compared with the corresponding FBP-based analogue. For carbon dioxide, solubility is increased by t-butyl group substitution but CO_2/CH_4 solubility and diffusivity selectivity both decline. The carbon dioxide solubility is lower for both PhAnth-based polyarylates but the CO_2/CH_4 solubility and diffusivity selectivities are both higher than for the corresponding FBP-based analogues. Thus, overall CO_2/CH_4 selectivity is higher for polyarylates based on PhAnth than on FBP.

Table 3 Mobility and solubility components of the O_2/N_2 separation factor[a]

Polymer	P_{O_2} (barrers)	$\alpha^*_{O_2/N_2}$	$\bar{S}_{O_2}$[b] (cm^3 (STP) cm^{-3} atm^{-1})	$\bar{S}_{O_2}/\bar{S}_{N_2}$	$\bar{D}_{O_2} \times 10^8$[c] ($cm^2$ s^{-1})	$\bar{D}_{O_2}/\bar{D}_{N_2}$
PhAnth/IA	2.05	5.74	0.57	1.46	2.73	3.94
PhAnth/tBIA	6.82	5.05	0.64	1.44	8.06	3.51
FBP/IA	3.03	5.32	0.76	1.40	3.05	3.79
FBP/tBIA	9.55	4.95	0.81	1.21	9.02	4.08

[a] Data at 35°C and 2 atm
[b] Calculated from the sorption isotherm
[c] Calculated from $D = P/S$

Table 4 Mobility and solubility components of the CO_2/CH_4 separation factor[a]

Polymer	P_{CO_2} (barrers)	$\alpha^*_{CO_2/CH_4}$	$\bar{S}_{CO_2}$[b] (cm^3 (STP) cm^{-3} atm^{-1})	$\bar{S}_{CO_2}/\bar{S}_{CH_4}$	$\bar{D}_{CO_2} \times 10^8$[c] ($cm^2$ s^{-1})	$\bar{D}_{CO_2}/\bar{D}_{CH_4}$
PhAnth/IA	9.0	27.0	3.29	3.39	2.08	7.95
PhAnth/tBIA	25.9	17.3	3.48	3.08	5.66	5.60
FBP/IA	12.4	20.1	3.56	2.97	2.65	6.81
FBP/tBIA	36.8	15.5	3.96	2.89	7.06	5.35

[a] Data at 35°C and 10 atm
[b] Calculated from the sorption isotherm
[c] Calculated from $D = P/S$

Table 5 Dual-mode sorption parameters at 35°C

Polymer	Gas	k_D (cm^3 (STP) cm^{-3} atm^{-1})	C'_H (cm^3 (STP) cm^{-3})	b (atm^{-1})
PhAnth/IA	N_2	0.113	3.47	0.096
	CH_4	0.216	12.4	0.156
	CO_2	0.968	29.6	0.362
PhAnth/tBIA	N_2	0.158	3.38	0.102
	CH_4	0.247	14.7	0.148
	CO_2	1.18	28.3	0.428

Previous studies have correlated the CO_2/CH_4 solubility selectivity of various polymers with the concentration of carbonyl or polar groups in the material[22]. Such a correlation for the PhAnth-based materials and a number of other polyarylates is shown in *Figure 10*. In general, higher carbonyl density enhances CO_2/CH_4 solubility selectivity. Dilution of carbonyl density by t-butyl substitution lowers CO_2/CH_4 solubility selectivity in all cases.

The sorption data are well described by the dual-mode sorption model[23,24]

$$C = k_D p + \frac{C'_H b p}{1 + bp} \quad (7)$$

where k_D is the Henry's law solubility coefficient, C'_H is the Langmuir capacity factor and b is an affinity parameter characterizing the relative rates of sorption and desorption. Non-linear curve fitting of the sorption data to the dual-mode sorption model gives the parameters listed in *Table 5*.

CONCLUSIONS

The gas sorption and transport properties of two polyarylates based on PhAnth have been described. Substitution of a t-butyl unit increases the gas permeability by two- to three-fold while decreasing the permselectivity. Gas sorption is moderately increased by t-butyl substitution; however, higher diffusion coefficients are the primary cause of the much higher gas permeabilities. The anthronylidene connector group leads to higher permselectivity, as compared with the fluorenylidene connector group, for all reported gas pairs, at the expense of permeability. Increased polar attractions between chains is the probable explanation for these effects, plus, for those separations involving CO_2, the interaction of CO_2 with the anthronylidene carbonyl unit.

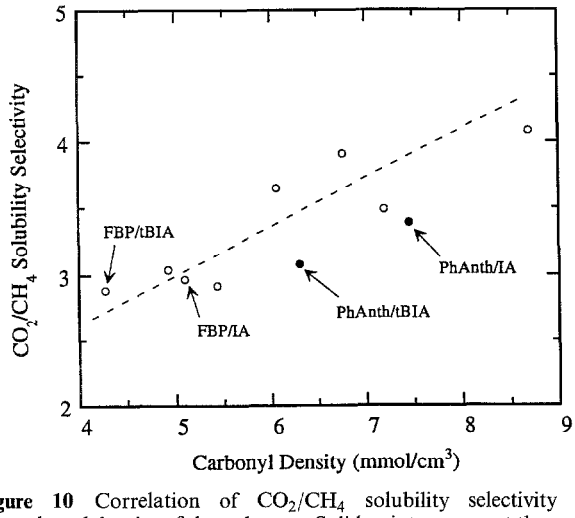

Figure 10 Correlation of CO_2/CH_4 solubility selectivity with the carbonyl density of the polymers. Solid points represent the current polyarylate data while open points correspond to various polyarylates described elsewhere[3]. The dotted line is the best linear fit of all the data

ACKNOWLEDGEMENTS

This research was supported by the Department of Energy, Basic Sciences Program, under Grant DE-FG05-86ER13507 and the Separations Research Program at The University of Texas at Austin. M.R.P. acknowledges the Phillips Petroleum Foundation for fellowship support.

REFERENCES

1 Korshak, V. V., Salazkin, S. N., Beridze, L. A. and Vinogradova, S. V. *Polym. Sci. USSR* 1973, **15**, 947
2 Morgan, P. W. *Macromolecules* 1970, **3**, 536
3 Pixton, M. R. and Paul, D. R. *J. Polym. Sci., Polym. Phys. Edn* 1995, **33**, 1135
4 Pixton, M. R. and Paul, D. R. *J. Polym. Sci., Polym. Phys. Edn* in press
5 Vinogradova, S. V., Salazkin, S. N., Beridze, L. A., Mzhel'skii, A. I., Askadskii, A. A., Slonimskii, G. L. and Korshak, V. V. *Polym. Sci. USSR* 1969, **11**, 27
6 Morgan, P. W. in 'Polymer Reviews' (Eds H. F. Mark and E. H. Immergut), Interscience Publishers, New York, 1965, p. 325
7 Morgan, P. W. in 'Macromolecular Syntheses' (Ed. W. J. Bailey), John Wiley & Sons, New York, 1972, p. 29
8 Koros, W. J., Paul, D. R. and Rocha, A. A. *J. Polym. Sci., Polym. Phys. Edn* 1976, **14**, 687
9 Jordan, S. M., Koros, W. J. and Fleming, G. K. *J. Membrane Sci.* 1987, **30**, 191
10 Raymond, P. C. and Paul, D. R. *J. Polym. Sci., Polym. Phys. Edn* 1990, **28**, 2213
11 Koros, W. J. and Paul, D. R. *J. Polym. Sci., Polym. Phys. Edn* 1976, **14**, 1903
12 Koros, W. J., Chan, A. H. and Paul, D. R. *J. Membrane Sci.* 1977, **2**, 165
13 Windle, A. H. *Pure Appl. Chem.* 1985, **57**, 1627
14 Aguilar-Vega, M. and Paul, D. R. *J. Polym. Sci., Polym. Phys. Edn* 1993, **31**, 1599
15 Bondi, A. 'Physical Properties of Molecular Crystals, Liquids, and Glasses', John Wiley & Sons, New York, 1968
16 Van Krevelen, D. W. 'Properties of Polymers', 3rd Edn, Elsevier Science Publishers, New York, 1990
17 McHattie, J. S., Koros, W. J. and Paul, D. R. *Polymer* 1991, **32**, 840
18 McHattie, J. S., Koros, W. J. and Paul, D. R. *Polymer* 1991, **32**, 2618

19 McHattie, J. S., Koros, W. J. and Paul, D. R. *Polymer* 1992 **33**, 1701
20 Aitken, C. L., Koros, W. J. and Paul, D. R. *Macromolecules* 1992, **25**, 3424
21 Aitken, C. L., Koros, W. J. and Paul, D. R. *Macromolecules* 1992, **25**, 3651
22 Koros, W. J. *J. Polym. Sci., Polym. Phys. Edn* 1985, **23**, 1611
23 Vieth, W. R., Howell, J. M. and Hsieh, J. H. *J. Membrane Sci.* 1976, **1**, 177
24 Barrer, R. M., Barrie, J. A. and Slater, J. *J. Polym. Sci.* 1958, **27**, 177